International Journal of Fluid Power 9 (2008) No. 2 pp. 5-13

DEVELOPMENT OF A DIRECT PRESSURE-SENSING WATER HYDRAULIC RELIEF VALVE

Kenji Suzuki and Eizo Urata

Department of Mechanical Engineering, Kanagawa University – Rokkakubashi 3-27-1, Kanagawa-ku, Yokohama 221-8686, Japan
suzuki@kanagawa-u.ac.jp, urata@kanagawa-u.ac.jp

Abstract

A balanced-piston-type water hydraulic relief valve working at a rated pressure of 14 MPa is developed. The design focuses on preventing cavitation and improving the static characteristics and stability. To prevent cavitation, the main valve has two throttles of nearly equal dimensions in series. As static characteristics, pressure override and hysteresis are considered. To reduce the pressure override, the supply pressure is directly led to the pilot valve. To reduce the hysteresis, the main valve is supported by hydrostatic bearings, which eliminate Coulomb friction in the main valve. To improve the stability of the main valve, a viscous damper is attached to the main valve besides inserting a damping orifice between the main- and the pilot valves. Simulation of static- and dynamic characteristics are carried out to determine the valve dimensions. The experimental results for a flow rate of up to 20 litres/min showed that the measured pressure override and hysteresis are about 1 % and 0.1 % of the pre-set pressure, respectively. The developed relief valve did not radiate cavitation noise in the range (maximum pressure 14 MPa) of the experiments.

Keywords: water hydraulics, relief valve, cavitation, pressure override, hysteresis, hydrostatic bearing

1 Introduction

Most water hydraulic valves have the same basic structure as those used in oil hydraulics. Such water hydraulic valves are produced using different materials and with slightly different dimensions to oil hydraulic valves, which somewhat improve rust prevention and wear resulting from the poor lubrication property of water (Trostmann, 1996). However, cavitation associated with the high vapour pressure of water and valve vibration induced by low viscous damping is difficult to resolve with such mild improvement of valve design.

To resolve all these problems, we must look for new design possibilities for water hydraulic valves. This paper submits a prototype water hydraulic relief valve that can be rated as a new design possibility. In this design, special attention is paid to four items: cavitation prevention, valve stiction avoidance, pressure override reduction, and damping improvement.

While cavitation is liable to occur in flow through throttles with high pressure-difference, a high pressure-difference across throttles in relief valves is usual. If a water hydraulic valve has the same dimensions as an oil hydraulic valve, it will often radiate cavitation noise and its service life will become shorter. Reducing pressure gradually by making complex paths in a valve throttle is effective for suppressing cavitation (Skousen, 1997), at the expense of larger valve dimensions. Another way to prevent cavitation is multi-stage pressure reduction (Berger, 1983; Liu et al., 2002). Dividing a high pressure into two or three stages is an effective way of reducing damage to valves, noise and vibration induced by cavitation. The design in this paper adopts two serial throttles for the main valve, as in the former designs of the present author (Suzuki and Urata, 2003, 2005a, 2005b).

The poor lubrication characteristic of water causes stiction between the valve and the sleeve. In the developed valve, the hydrostatic bearings are built into the sliding part of the main valve for smoother motion. In a conventional balanced-piston-type relief valve, fluid flows from supply pressure port to the pilot pressure chamber through a capillary (Cundiff, 2001). In the developed valve, the flow through the hydrostatic bearing is directed to the pilot pressure chamber; thus it is used as the pilot flow, and the capillary in the classical design is not adopted. Using the clearance of the sliding part as a restrictor has been successfully adopted in other water hy-

This manuscript was received on 26 February 2008 and was accepted after revision for publication on 16 June 2008

draulic valves, such as a servovalve (Urata et al., 1998) and a high-speed solenoid valve (Park et al., 2004).

To reduce pressure override, some authors' designs directed the supply pressure to the pilot valve and detected the supply pressure directly (Andersson, 1984; Yao et al., 1997; Suzuki and Urata, 2003, 2005a). However, application of this design principle resulted in violent resonance of the relief valve with pulsation of the supply pump.

To prevent such vibration, a damping orifice was inserted between the main- and pilot valves (Suzuki and Urata, 2005b). However, the damping orifice showed only a limited effect. Therefore, in the present design, besides the damping orifice, a viscous damper is attached to the main valve so as the valve provides the necessary attenuation characteristic.

This water hydraulic relief valve was designed to work at a rated pressure of 14 MPa. The dimensions of the valve were determined based on numerical simulations of the static and dynamic characteristics. Experiments for the static characteristic at a flow rate of up to 20 litres/min were conducted and the relief valve performance, namely, pressure-flow characteristics, pressure override and hysteresis was investigated.

2 Structure of the Designed Valve

Figure 1 shows a cross-section of the developed valve. The mounting surface dimensions agree with ISO code: 6264-06-09-1-97. The valve body and most of the inner parts are made of copper alloy and stainless steel, respectively. The main valve is made of aluminium bronze, which has a high resistance to cavitation erosion (Suzuki and Urata, 2002). Definitions of the functions and dimensions of the main- and pilot valve are given in Fig. 2(a) and (b), respectively. The reference dimensions of the valve are shown in Table 1. These dimensions were determined based on the design analysis described in Section 3.

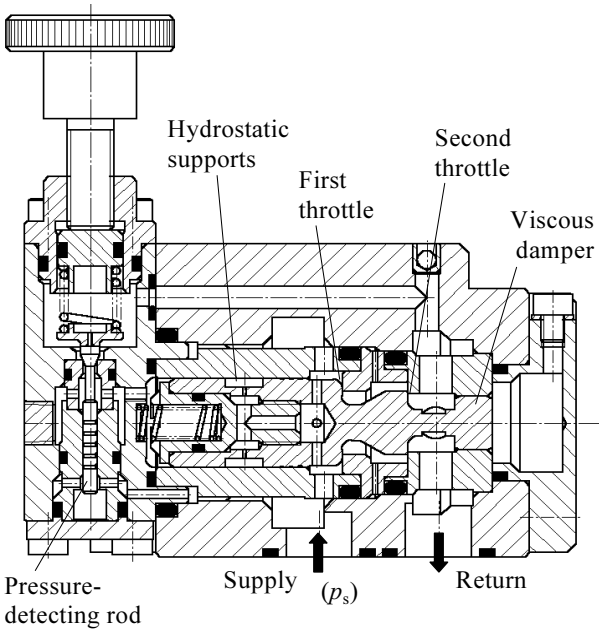

Fig. 1: *Cross-section of the developed valve*

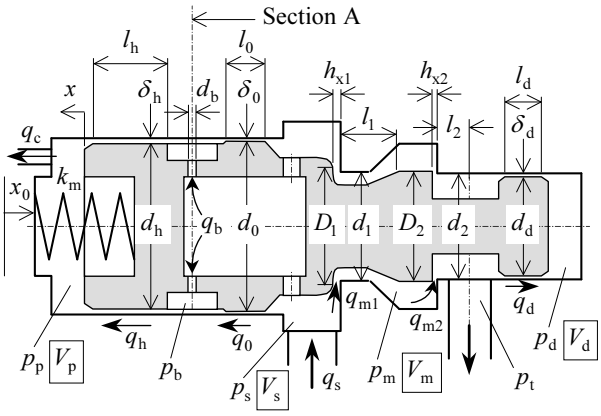

(a) Main valve

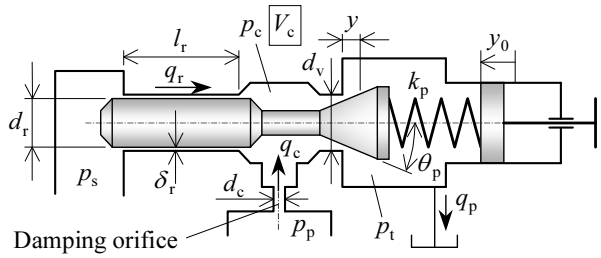

(b) Pilot valve

Fig. 2: *Valve functions and dimensions*

Table 1: Reference dimensions of the developed valve

Main valve					
D_1	15 mm	d_1	14.2 mm	h_{01}	5 μm
D_2	13.77 mm	d_2	13.1 mm	h_{02}	0.5 μm
d_d	11.99 mm	l_d	6 mm	δ_d	10 μm
k_m	0.49 N/mm	x_0	19 mm	d_c	1 mm
V_m	1.73 cm^3	V_{d0}	5.16 cm^3	m_m	94 g
Hydrostatic supports					
d_h	19.975 mm	l_h	11 mm	δ_h	17.5 μm
d_0	19.99 mm	l_0	5.4 mm	δ_0	10 μm
d_b	0.6 mm	N_b	4		
Pilot valve					
d_r	2.99 mm	l_r	10 mm	δ_r	10 μm
k_p	22.9 N/mm	d_v	3.01 mm	θ_p	20 deg
V_c	1.06 cm^3	V_{p0}	1.31 cm^3	m_p	5 g

The main valve has two serial throttles formed with parallel annular planes. Although their diameters are almost equal, d_1 is a little greater than D_2 for convenience of assembling.

To accurately determine the axial distance between the two throttles, the valve sleeve is made of three pieces. The axial length of the central piece of the sleeve, which provides the first valve-seat, is made slightly shorter than the distance between the two sealing faces of the main valve. Therefore, when the displacement of the main valve is zero, i.e., the second

throttle is closing, and the first throttle is opening slightly.

Commonly adopted serial throttles are such that valve seats contact conical surfaces of the valve with two circular lines (Liu et al., 2002; Suzuki and Urata, 2003; Nie et al., 2006; Lauttamus et al., 2006). However, simultaneous contact of two edges of the valve seats is almost impossible to achieve by industrial manufacturing. Moreover, the contact lines are flattened and the characteristics of the valve change in a very short operating time. Therefore, plane contact is adopted for both throttles in the present design. The planes are made perpendicular to the valve axis. Therefore, the jet angle of the flow becomes almost perpendicular to the valve axis.

The main valve is supported by hydrostatic bearings for smoother motion. The hydrostatic support is shown in Fig. 3 which illustrates a cross-section of section A from Fig. 2. In Fig. 3, water passes through the bearing orifices, recesses, and the clearance between the valve and the sleeve, and flows to the pilot chamber. Thus, the hydrostatic support is also used as a restrictor from the supply pressure to the pilot pressure.

For the hydrostatic support, four recesses are placed with circumferentially equal intervals. When the position of the main valve deviates from the centre of the sleeve, the pressures in the recesses in the direction of the deviation increase; simultaneously, the pressures at the other side decrease. Consequently, a restoring force is generated which pushes the main valve back to the central position. To magnify the restoring force, the clearance around the main valve has a stepwise change in its axial direction, namely, $\delta_h > \delta_0$.

In the pilot valve, a pressure-detecting rod is attached to the tip of the conical poppet valve. The supply pressure that pushes the left end of the rod is balanced by the pilot spring pushing the right end of the poppet valve. Thus, the pilot valve detects the supply pressure directly.

To improve stability of the main valve, a viscous damper is attached to the main valve besides inserting a damping orifice between the main- and the pilot valves.

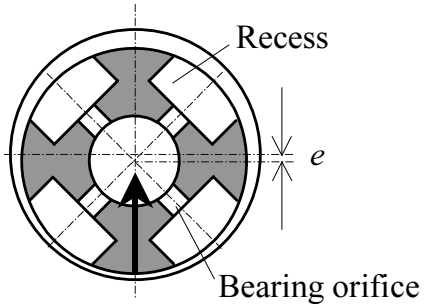

Fig. 3: *Hydrostatic support*

3 Analysis for Design

To determine the dimensions of the valve, a design analysis was carried out. The following assumptions were made to simplify the basic equations:

- Flow through a narrow annular clearance is regarded as laminar between parallel planes.
- The viscous drag force acting on the valve due to leakage flow is negligibly small compared to forces exerted by pressures and springs.
- The throttles of the main valve are composed of smooth parallel planes; thus, the influence of surface irregularity of the contact plane on the leakage is ignored.
- In the throttles of the main valve, water flows along the wall; thus, contraction of the flow is not considered.
- Cavitation does not occur at the valve throttles.
- Flow through the main valve throttles become almost perpendicular to the valve axis; thus, the flow force acting on the main valve can be ignored.
- Elastic deformation of valve parts is small and can be ignored.
- Return port pressure is negligibly smaller than the intermediate pressure and the supply pressure.

3.1 Flow Rate through the Hydrostatic Supports

Flow through the circumferential clearance of the hydrostatic bearings can be estimated by numerical analysis (Suzuki and Urata, 1999). However, it requires a long calculation time; it is inconvenient for design analysis in that various combinations of parameters have to be tried. In the design of this valve, therefore, we used an approximate calculation explained below.

The flow through the circumferential clearance of the hydrostatic bearings varies when the main valve deviates from the axially concentric position. However, the restoring force pushes it back to the concentric position. In the steady state, therefore, it lies near the concentric position. Therefore, the flow through the annular clearance is estimated for the concentric position.

The recesses make a complex boundary in the clearance space. To simplify the flow rate calculation, the spread of the recess areas is ignored and the orifice flow is approximated by the flow from a line source put at the position of section A in Fig. 2. Under this simplification, flow rates through the bearing orifices and the clearances can be written as follows.

$$q_b = K_b\sqrt{p_s - p_b} \tag{1}$$

$$q_0 = K_0(p_s - p_b) \tag{2}$$

$$q_h = K_h(p_b - p_p) \tag{3}$$

where

$$K_b = N_b c_{db}\frac{\pi}{4}d_b^2\sqrt{\frac{2}{\rho}},\ K_0 = \frac{\pi d_0\delta_0^3}{12\mu l_0},\ K_h = \frac{\pi d_h\delta_h^3}{12\mu l_h} \tag{4}$$

and c_{db} is the discharge coefficient of the bearing orifice.

The continuity equation is

$$q_h = q_0 + q_b \tag{5}$$

Combining Eq. 1 to 5 yields

$$q_0 = \frac{K_0}{K_b^2} q_b^2, \quad q_b = \frac{-K_2 + \sqrt{K_2^2 + 4K_1(p_s - p_p)}}{2K_1} \tag{6}$$

where

$$K_1 = \frac{1}{K_b^2}\left(1 + \frac{K_0}{K_h}\right), \quad K_2 = \frac{1}{K_h} \tag{7}$$

Thus, the flow rate q_h is found by Eqs. 5 and 6 when Δp ($= p_s - p_p$) is given.

Figure 4 compares the numerical calculation and the above-approximated analysis. The flow rate by the above-approximation is about ten percent greater than the results of the numerical analysis. This accuracy is sufficient for screening of parameter selection; hence, the approximate calculation was used for selection of the design parameters and the numerical calculation was applied for the finally selected dimensions.

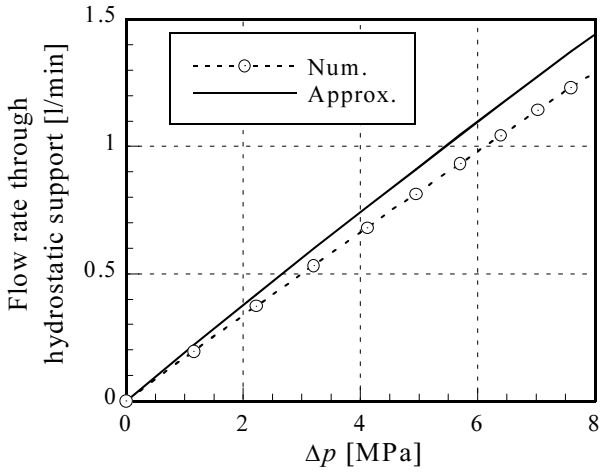

Fig. 4: *Pressure-flow rate characteristics of the hydrostatic supports*

3.2 Flow through Restrictors

This sub-section is concerned with basic equations except for the hydrostatic supports. The flow rates through the restrictors are as follows.

$$q_{m1} = c_{d1}\pi D_1 h_{x1}\sqrt{2(p_s - p_m)/\rho} \tag{8}$$

$$q_{m2} = c_{d2}\pi D_2 h_{x2}\sqrt{2(p_m - p_t)/\rho} \tag{9}$$

$$q_c = \mathrm{sgn}(p_p - p_c) c_{dc}\frac{\pi}{4} d_c^2\sqrt{2|p_p - p_c|/\rho} \tag{10}$$

$$q_p = c_{dp}\pi d_v y \sin\theta_p\sqrt{2(p_c - p_t)/\rho} \tag{11}$$

$$q_r = \frac{\pi d_r \delta_r^3}{12\mu l_r}(p_s - p_c) \tag{12}$$

$$q_d = \frac{\pi d_d \delta_d^3}{12\mu l_d}(p_t - p_d) \tag{13}$$

where c_{d1}, c_{d2}, c_{dc} and c_{dp} are the discharge coefficients of the first and second throttles of the main valve, the damping orifice and the poppet valve, respectively.

The axial clearances of the first and second throttles of the main valve are

$$h_{x1} = h_{01} + x, \;\; h_{x2} = h_{02} + x \tag{14}$$

respectively, because the valve is assumed to be a rigid body.

3.3 Dynamic Equations

To determine the dimensions of the damping mechanism, dynamic analysis is necessary even though the dynamic characteristics of the valve are not the research object of this study. This sub-section derives the equations of motion of the valve.

Each throttle of the main valve makes a plane contact with the valve seats; thus, lapped areas are formed between the valve and the valve seats. The pressure distribution in the lapped area can influence the force acting on the main valve. However, the radial length of the lapped area in the developed valve is very short (about 0.4 mm). Under this geometry, a reasonable simplification is to assume that the pressure in the lapped area is equal to the downstream pressure of each throttle. Then, the equations of motion for the main- and pilot valves are

$$\begin{aligned}&(m_m + m_{fm})\frac{d^2x}{dt^2} + C_m\frac{dx}{dt} + k_m(x + x_0) - \rho L\frac{dq_m}{dt} \\ &= A_s p_s + A_m p_m + A_t p_t + A_d p_d - A_p p_p\end{aligned} \tag{15}$$

and

$$\begin{aligned}&(m_p + m_{fp})\frac{d^2y}{dt^2} + C_p\frac{dy}{dt} + k_p(y + y_0) \\ &= A_r p_s + (A_v - A_r)p_c - K_{fp}y(p_c - p_t)\end{aligned} \tag{16}$$

respectively, where

$$\left.\begin{aligned}&A_s = \tfrac{\pi}{4}\left(d_h^2 - D_1^2\right),\ A_m = \tfrac{\pi}{4}\left(D_1^2 - D_2^2\right), \\ &A_t = \tfrac{\pi}{4}\left(D_2^2 - d_d^2\right),\ A_d = \tfrac{\pi}{4}d_d^2,\ A_p = \tfrac{\pi}{4}d_h^2, \\ &A_r = \tfrac{\pi}{4}d_r^2,\ A_v = \tfrac{\pi}{4}d_v^2,\ L = l_1 + l_2\end{aligned}\right\} \tag{17}$$

$$C_m = \pi\mu\left(\frac{d_0 l_0}{\delta_0} + \frac{d_h l_h}{\delta_h} + \frac{d_d l_d}{\delta_d}\right),\ C_p = \pi\mu\frac{d_r l_r}{\delta_r} \tag{18}$$

$$K_{fp} = c_{dp}\pi d_v \sin 2\theta_p \tag{19}$$

Equation 15 indicates that a smaller value of A_m is desirable to minimise the influence of p_m on the motion of the main valve. Although A_m cannot be zero because assembling of the valve requires $D_1 > D_2$, the difference of these diameters was made as small as possible.

Since flow is inward at the throttles of the main valve, damping lengths l_1 and l_2 generate a negative damping force. In simulation, however, the magnitude of the negative damping force (the fourth term on left side of Eq. 15) became less than 1 % of damping force generated by the viscous damper ($A_d p_d$: the fourth term on right side of Eq. 15). Therefore, the influence of the damping length is overcome in this design.

On the right side of Eq. 16, the second term is ignored because $d_r \approx d_v$. Next, the third term, which expresses flow force, is much smaller than the first term since the pilot flow rate is small and $y \ll d_v$. Therefore, the position of the pilot valve is mainly influenced by

the forces of the supply pressure and the pilot spring. Consequently, the position of the pilot valve can be used to detect the supply pressure with very small error.

Finally, we consider the equations of continuity. The volumes V_s, V_m and V_c, whose pressures are p_s, p_m and p_c, respectively, are regarded as constants because their relative changes caused by the motion of the valve are small. Considering the compressibility of water, the equations of continuity are as follows.

$$\frac{dp_s}{dt} = \frac{\beta}{V_s}\left(q_s - q_{m1} - q_h - q_r - A_s\frac{dx}{dt} - A_r\frac{dy}{dt}\right) \quad (20)$$

$$\frac{dp_m}{dt} = \frac{\beta}{V_m}\left(q_{m1} - q_{m2}\right) \quad (21)$$

$$\frac{dp_p}{dt} = \frac{\beta}{V_{p0} - A_p x}\left(q_h - q_c + A_p\frac{dx}{dt}\right) \quad (22)$$

$$\frac{dp_c}{dt} = \frac{\beta}{V_c}\left(q_r + q_c - q_p\right) \quad (23)$$

$$\frac{dp_d}{dt} = \frac{\beta}{V_{d0} + A_d x}\left(q_d - A_d\frac{dx}{dt}\right) \quad (24)$$

where V_{p0} and V_{d0} are the initial values of V_p and V_d at $x = 0$, respectively.

3.4 Simulation

In the simulation at design stage of the valve, the discharge coefficients of restrictors were assumed to be constant of 0.67. This assumption could bring inaccuracy to calculation results for a smaller flow rate. More precise modelling of discharge coefficient would be required for more accurate simulation.

The static characteristics of the relief flow rate are obtained as the numerical solution of Eq. 5 to 24 eliminating the time-derivative terms. Supply pressure or flow rate through the main valve was given as an input parameter. The other unknown parameters are found by solving the steady-state equations using the bisection method.

Figure 5 shows the calculation results of the supply pressure at the relief flow rate of 20 l/min up to 14 MPa by each 1 MPa. The pilot valve opened with the rise of the supply pressure, and the supply pressure became almost constant after the main valve opened at the cracking pressure. The calculated pressure overrides were less than 0.4 %, except for the pre-set pressure of 1 MPa.

To determine the size of the damper, response of the pressure to stepwise change of the relief flow rate was calculated. The MATLAB/Simulink® was used for the modelling of Eq. 5 to 24. The Runge-Kutta method of fourth-order was used as the solver. The time step for calculation was a fixed step of 5 μs. A stepwise change of flow rate of 1.5 to 20 l/min was used as the input signal. The fluid volume upstream of the relief valve was adjusted to be equal to that of the experimental rig because it has a critical influence on the transient response. The response of the supply pressure was calculated for initial values of 7 and 14 MPa, changing dimensions of the damper of the main valve and the damping orifice.

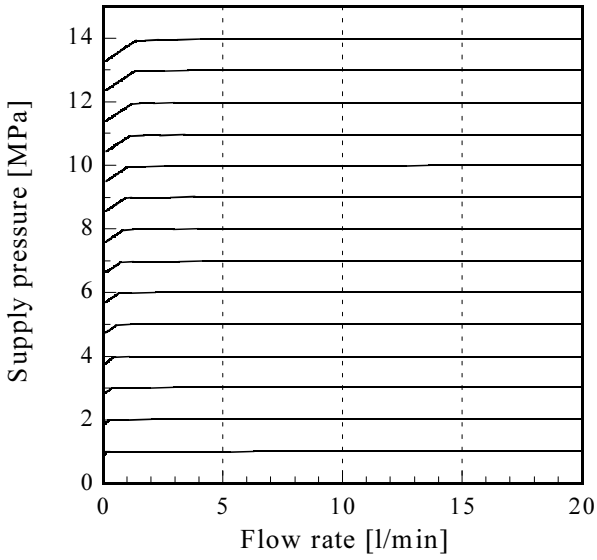

Fig. 5: *Simulation results of static characteristics*

The pressure response with and without the damper for the main valve is shown in Fig. 6. The diameter of the damping orifice is 1 mm for both cases. Figure 6 indicates the importance of the damper; it also reveals that the pressure oscillation attenuates more slowly for higher supply pressure.

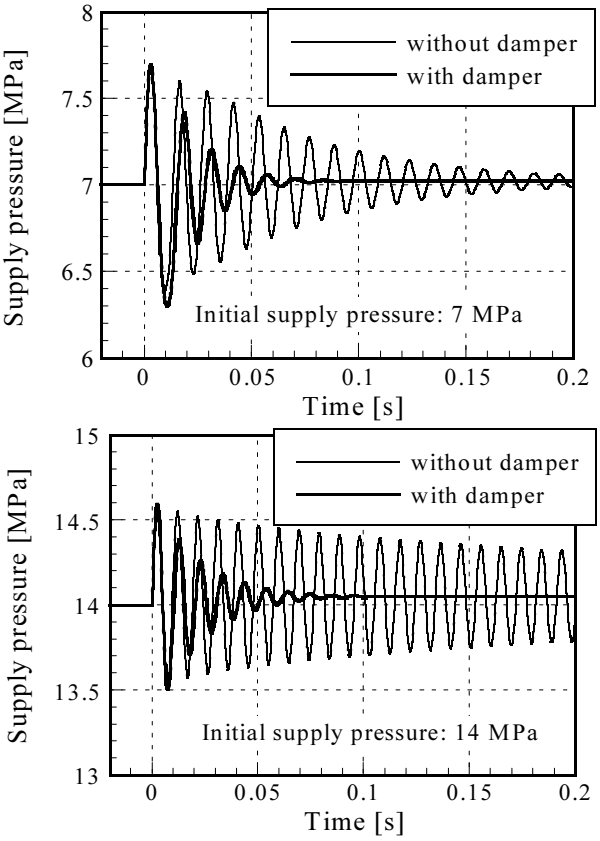

Fig. 6: *Simulation results of dynamic response with and without damper for the main valve*

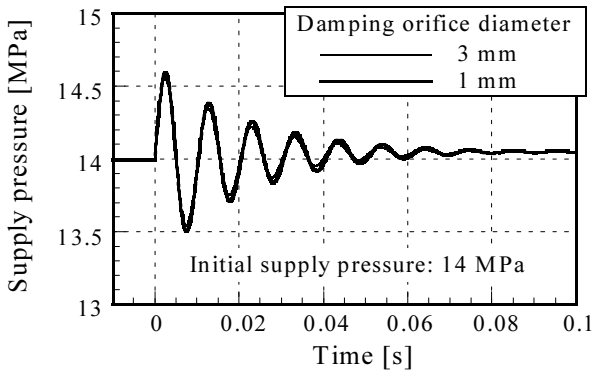

Fig. 7: *Simulation results of dynamic response with and without damping orifice*

Through experiments, it has been recognised that a damping orifice was more effective in suppressing the valve vibration caused by flow pulsation of the pump. However, the simulation (Fig. 7) indicates that the selection of the orifice diameter is not critical to the damping of the transient pressure.

4 Experiment

4.1 Experimental Rig

Figure 8 illustrates the experimental rig. A three-throw piston pump with an accumulator was used as the water pressure source. The rated pressure is 21 MPa and the rated flow rate is 20 l/min. The flow to the test relief valve was adjusted by controlling a bypass flow with a manually operated needle valve connected parallel to the test relief valve. The relief flow rate was measured by switching two kinds of turbine-type flow meters with different ranges. Thus, the accuracy of flow measurement is made about 2 percent. The resolution of the pressure measurement system was about 10 kPa. The water temperature was kept at 25 – 30 C by a cooler in the return-line to the reservoir.

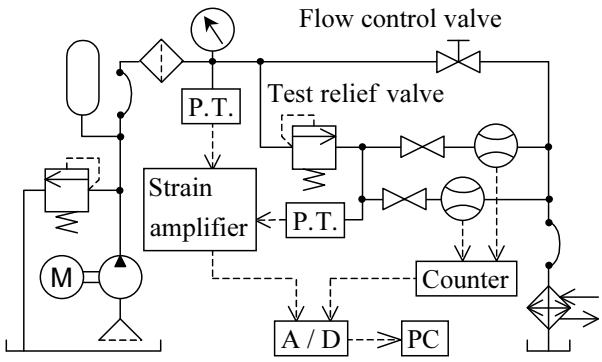

Fig. 8: *Experimental rig*

4.2 Experimental Results

Figure 9 shows the experimental results for the supply pressure up to 14 MPa by each 1 MPa. The white data points and black ones are for the increase and decrease of flow rate, respectively. The solid lines are the simulation results shown in Fig. 5. Difference between the simulation and the experiment is observed only for pressures less than cracking pressures.

The pressure override by the experiment and by the simulation is compared in Fig. 10. The indicated pressure override is (pressure at the maximum flow rate) – (the cracking pressure). Figure 10 also shows the percentile override that is given by dividing the override by the pre-set pressure. As observed from Fig. 10, the pressure override is about 1% of the pre-set pressure.

Figure 11 shows the dimensionless pressure hysteresis observed by the experiment. The percentile hysteresis is defined by

$$H = \frac{|p_{\mathrm{I}} - p_{\mathrm{D}}|}{p_{\mathrm{I}} + p_{\mathrm{D}}} \times 100 \qquad (25)$$

The average of the dimensionless hysteresis is about 0.1 % over a pre-set pressure range from 2 to 14 MPa. An exception in Fig. 11 is the value at 1 MPa. This exception is caused by measurement uncertainty (10 kPa) that is very low compared to the rated operating pressure (14 MPa). The small value of hysteresis indicates that the main valve moved smoothly by the hydrostatic supports.

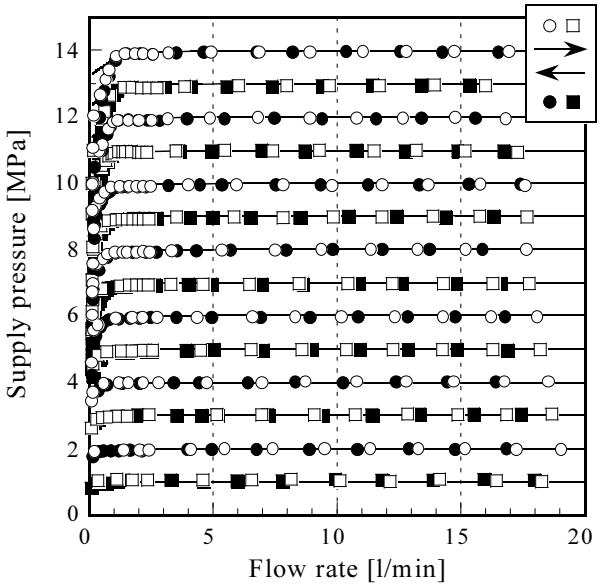

Fig. 9: *Experimental results of static characteristics*

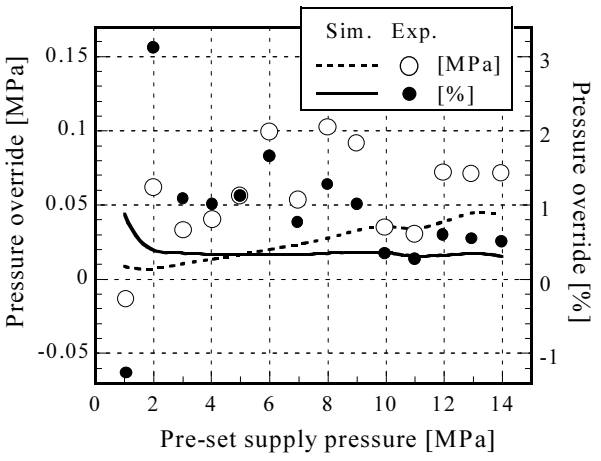

Fig. 10: *Pressure override*

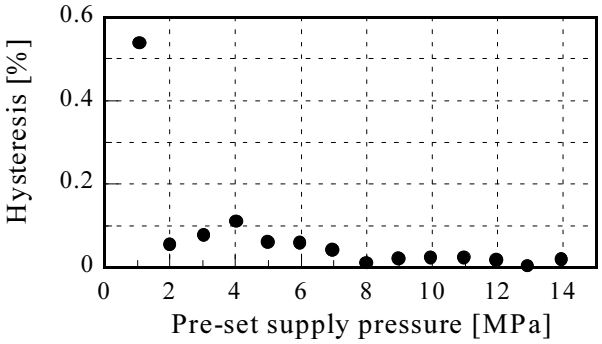

Fig. 11: *Experimental results of hysteresis*

The developed valve did not radiate cavitation noise in the range of experiment, which indicates that cavitation occurrence was prevented. This would be achieved by the effect of two-stage pressure reduction. More detail will be discussed in the next section.

5 Discussion

The main valve has two throttles to establish two-step pressure drops. The effect of the throttles can be observed through examining the intermediate pressure. The ideal value of the intermediate pressure satisfies $(p_m - p_t)/(p_s - p_t) = 0.5$. However, it is hardly established in practice because it requires completely simultaneous closing of the two throttles. To avoid uncertainty of cracking pressure, this design was intended preferential closing of the second throttle.

With this design principle, the second throttle is closing while the first throttle is opening when inlet pressure is lower than the cracking pressure. At this state, the intermediate pressure is equal to the inlet pressure; namely, the dimensionless intermediate pressure is unity. When the main valve moves from the cracking position, water flows through the valve and pressure drops at the first throttle. Simultaneously, the dimensionless intermediate pressure decreases. It shall approach a value determined by the ratio of the diameter of the throttles. Figure 12 compares the dimensionless intermediate pressure by experiment and simulation for typical pre-set pressures. Although the discrepancy between experiment and simulation is relatively large, it proves effective pressure reduction by the two throttles. The cause of the discrepancy may include an inaccurate estimate of the discharge coefficient, insufficient surface accuracy of the mating planes, or elastic deformation of valve parts.

The pressure-flow characteristic shows small pressure override and fine agreement between simulation and experiment, despite insufficient agreement for the intermediate pressure. This can be explained as the result of direct sensing of the supply pressure by the pilot valve. The supply pressure is balanced by a spring and the disturbance is the flow force on the pilot valve while the pilot flow is independent of the intermediate pressure. Therefore, the intermediate pressure does not influence the pressure-flow characteristic.

The intermediate pressure may influence stability of the valve because it may change the flow force on the main valve. In this design, we avoided study in this direction and the stability was provided by addition of the damper to the main valve.

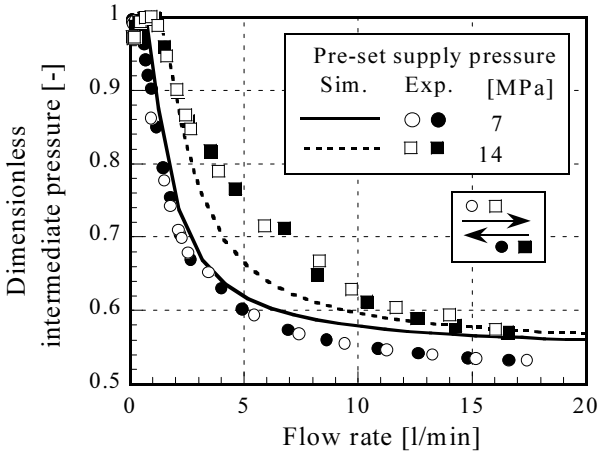

Fig. 12: *Dimensionless intermediate pressure in the space between two throttles of the main valve*

6 Conclusion

A balanced-piston-type water hydraulic relief valve working at a rated pressure of 14 MPa is developed. To prevent cavitation, the main valve has two throttles in series. The developed relief valve does not radiate cavitation noise in the range of the experiments. The main valve is supported by a hydrostatic bearing, in which the annular clearance between the valve and the sleeve is used as a restrictor for the pilot pressure. To reduce the pressure override, the pilot valve directly detects the supply pressure. To obtain the stability of the valve, a viscous damper is attached to the main valve besides inserting a damping orifice between the main- and the pilot valves. Numerical simulation of the dynamic and static characteristics is carried out to determine the valve dimensions.

The experiment at a flow rate of up to 20 litres/min shows that the pressure override is about 1 % of the pre-set pressure. The experiment also shows that the hysteresis is about 0.1 % of the pre-set pressure; thus the smooth motion of the main valve by the hydrostatic supports is confirmed.

Nomenclature

A_*	areas (see Eq. 17)	[m^2]
c_{d*}	discharge coefficients of restrictors	[-]
c_{db}	discharge coefficient of the bearing orifice	[-]
C_m, C_p	damping coefficient of main- and pilot valves, respectively	[Ns/m]
d_*	diameters (see Fig. 2)	[m]
D_i	external diameter of the i-th throttle of main valve	[m]
e	eccentricity of main valve to sleeve (see Fig. 3)	[m]
H	dimensionless hysteresis (see Eq. 25)	[-]
h_{xi}	axial opening of the i-th throttle of main valve	[m]
h_{0i}	initial axial clearance of the i-th throttle of main valve	[m]
K_*	constants (see Eq. 4, 7 and 19)	
k_m, k_p	spring constant of main- and pilot valves, respectively	[N/m]
L	damping length of main valve	[m]
l_*	length (see Fig. 2)	[m]
m_m, m_p	equivalent mass of main- and pilot valves, respectively (incl. 1/3 of corresponding spring mass)	[kg]
m_{fm}, m_{fp}	water mass moving with main- and pilot valves, respectively	[kg]
p_*	pressures (see Fig. 2)	[Pa]
p_D	supply pressure observed by decrease of relief flow rate	[Pa]
p_I	supply pressure observed by increase of relief flow rate	[Pa]
p_m	intermediate pressure (see Fig. 2)	[Pa]
q_*	flow rate (see Fig. 2)	[m^3/s]
t	time	[s]
V_*	volumes (see Fig. 2)	[m^3]
V_{d0}	initial value of V_d at $x = 0$	[m^3]
V_{p0}	initial value of V_p at $x = 0$	[m^3]
x	displacement of main valve	[m]
x_0	initial compression of main spring	[m]
y	displacement of pilot poppet valve	[m]
y_0	initial compression of pilot spring	[m]
β	bulk modulus of water	[Pa]
δ_*	radial heights of annular clearances (see Fig. 2)	[m]
Δp	pressure drop across hydrostatic supports ($= p_s - p_p$)	[Pa]
μ	viscosity of water	[Pa·s]
ρ	density of water	[kg/m^3]
θ_p	half cone angle of pilot poppet	[-]

References

Andersson, B. R. 1984. *On the Valvistor, a proportional controlled seat valve*. Dissertation. Linköping University.

Berger, J. 1983. *Kavitationserosion und Maßnahmen zu ihrer Vermeidung in Hydraulikanlagen für HFA-Flüssigkeiten*. Dissertation. RWTH Aachen.

Cundiff, J. S. 2001. *Fluid power circuits and controls: fundamentals and applications*. CRC Press.

Lauttamus, T., **Linjama, M.**, **Nurmia, M.** and **Vilenius, M.** 2006. A Novel Seat Valve with Reduced Axial Forces. *Bath workshop on Power Transmission and Motion Control*. Bath, UK.

Liu, Y. S., **Huang, Y.** and **Li, Z. Y.** 2002. Experimental investigation of flow and cavitation characteristics of a two-step throttle in water hydraulic valves. *Proc. Instn Mech Engrs, Part A: J. Power and Energy*, Vol. 216, pp. 105-111.

Nie, S., **Huang, G.**, **Li, Y.**, **Yang, Y.** and **Zhu, Y.** 2006. Research on low cavitation in water hydraulic two-stage throttle poppet valve. *Proc. Instn Mech Engrs, Part E: J. Process Mechanical Engineering*, Vol. 220, pp. 167-179.

Park, S.-H., **Kitagawa, A.** and **Kawashima, M.** 2004. Water hydraulic high-speed solenoid valve, Part 1: development and static behaviour. *Proc. Instn Mech Engrs, Part I: J. Systems and Control Engineering*, Vol. 218, pp. 399-409.

Skousen, P. L. 1997. *Valve handbook*. McGraw-Hill.

Suzuki, K. and **Urata, E.** 1999. Analysis of Hydrostatic Bearing for Water Hydraulic Servovalve, *6th Scandinavian Intl. Conf. on Fluid Power*. Tampere, Finland.

Suzuki, K. and **Urata, E.** 2002. Cavitation erosion of materials for water hydraulics. *Bath workshop on Power Transmission and Motion Control*. Bath, UK.

Suzuki, K. and **Urata, E.** 2003. Improvement of Cavitation Resistive Property of a Water Hydraulic Relief Valve. *8th Scandinavian Intl. Conf. on Fluid Power*. Tampere, Finland.

Suzuki, K. and **Urata, E.** 2005a. Improvement in Static Characteristics of a Water Hydraulic Relief Valve. *9th Scandinavian Intl. Conf. on Fluid Power*. Linköping, Sweden.

Suzuki, K. and **Urata, E.** 2005b. Dynamic Characteristics of a Direct-Pressure Sensing Water Hydraulic Relief Valve. *6th JFPS Intl. Symposium on Fluid Power*. Tsukuba, Japan.

Trostmann, E. 1996. *Water hydraulics control technology*. Dekker.

Urata, E., **Miyakawa, S.**, **Yamashina, C.**, **Nakao, Y.**, **Usami, Y.** and **Shinoda, M.** 1998. Development of a Water Hydraulic Servovalve, *JSME Intl. J., Ser. B*, Vol.41(2), pp. 286-294.

Yao, D., **Burton, R.**, **Nikiforuk, P.**, **Ukrainetz, P.** and **Zhou, Q.** 1997. Research and Development of a Direct Pressure Sensing Relief Valve. *4th Intl. Conf. on Fluid Power Transmission and Control*. Hangzhou, China.

Kenji Suzuki
Born in November 1969. After receiving his M. Sc. from Kanagawa University in 1995, he had worked at a motor industrial company for 3 years. In the company, he had engaged in development of hydraulic power steering gearboxes. Since 1998, he has worked as a research associate of Mechanical Engineering, Kanagawa University. His research interest is development of water hydraulic systems.

Eizo Urata
Born on April 23rd 1939 Tokyo (Japan). Graduated Tokyo Metropolitan University in 1963, Received doctoral degree from Tokyo Institute of Technology in 1972, Scholarship of Alexander von Humboldt Stiftung for November 1974-Februaly 1976 (RWTH Aachen by Prof. Backé). Research associate at Tokyo Institute of Technology 1963-1981, Associate professor at Kanagawa University 1981-1987, Professor 1987-today. Research area: Water Hydraulics.